Effects of Injection Schedule in Simulations of Injection Induced Seismicity

Kayla A. Kroll, Keith B. Richards-Dinger, James H. Dieterich, Joshua A. White
kroll5@llnl.gov keithrd@ucr.edu dieterichj@ucr.edu white230@llnl.gov
NRAP National Risk Assessment Partnership
Lawrence Livermore National Laboratory
UC Riverside, University of California

LLNL_POST-689442
Portions of this work were performed by Lawrence Livermore National Laboratory for the Department of Energy under contract number DE-AC52-07NA27344

Time-Dependent Earthquake Failure: Rate- and State-dependent Friction

$$\tau = \mu(\sigma - p)$$ 1) Coulomb failure criterion

$$\mu = \mu_0 + a\ln\left(\frac{V}{V^*}\right) + b\ln\left(\frac{\theta V^*}{D_c}\right)$$ 2) Rate- and State-dependent frictional coefficient

$$\tau = (\sigma - p)\left[\mu_0 + a\ln\left(\frac{V}{V^*}\right) + b\ln\left(\frac{\theta V^*}{D_c}\right)\right]$$ 3) Constitutive law

μ_0: Nominal coefficient of friction
V^*: Reference slip rate
V: Earthquake slip rate
θ: State variable
D_c: Characteristic slip distance
a and b: Constitutive parameters describing the material

Simulating Earthquakes with the Physics-based Earthquake Simulator, RSQSim

- Comprehensive simulation of fault slip phenomena:
  - → Earthquakes, continuous creep, slow slip events, afterslip, and tremor.
- Implements rate-and state-dependent friction effects
  - → Earthquake clustering effects: (i.e. aftershocks and foreshocks).
- High resolution models of geometrically complex fault systems:
  - → Up to10^6 fault elements.
  - → Range of earthquake magnitudes M3.5 to M8 (for 1 km^2 triangular elements).
- Highly efficient code
  - → Good statistical characterizations from long simulations of 10^6 earthquakes.
  - → Repeated simulations to explore parameter space.

Figure 1:

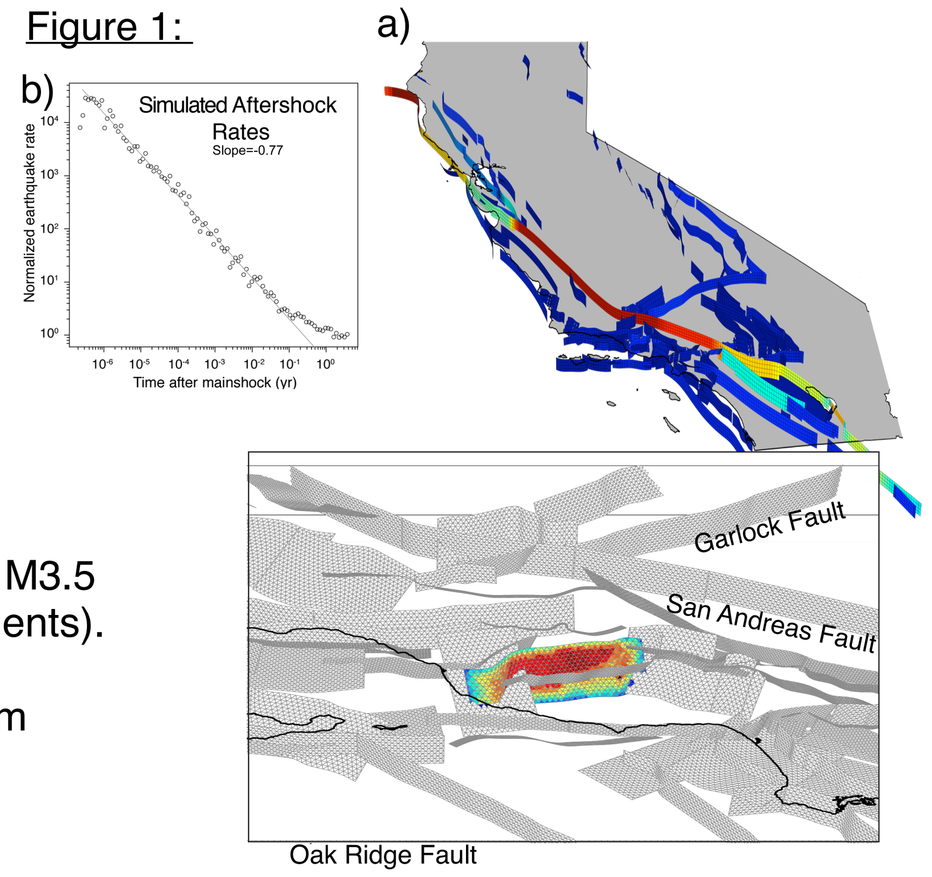

Figure 1: Example of an All-California (Ward, 2010) fault model used by RSQSim for earthquake simulations. b) Example of simulated aftershock rates that display Omori-like decay properties.

Incorporating Pore-fluid Pressure Changes in RSQSim

- RSQSim itself knows nothing of pore-fluid pressure diffusion, poroelastic effects, etc.
- Must supply external stressing history
- Geomechanical reservoir model
  - Changes in effective normal stress
  - Poroelastic effects
- Not fully coupled – no feedback
  - Seismic slip does not affect the permeability structure, etc.

- Linear diffusion model based on the analytical solutions for a point source in a semi-infinite, isotropic half-space (Eq. 4 and 5 by Wang, 2000).
- Variable injection parameters:
  - → Well location(s)
  - → Injection Rate
  - → Hydraulic diffusivity (K)

$$\Delta P = \left(\frac{V}{4\phi c(\pi k t)^{3/2}}\right)\exp\left(-\frac{r^2}{4\kappa t}\right) \quad (4) \qquad \left(\kappa = \frac{k}{\eta\phi c}\right) \quad (5)$$

V: Injection Volume
c: Compressibility
k: Permeability
ϕ: Porosity
η: Viscosity

Figure 2:

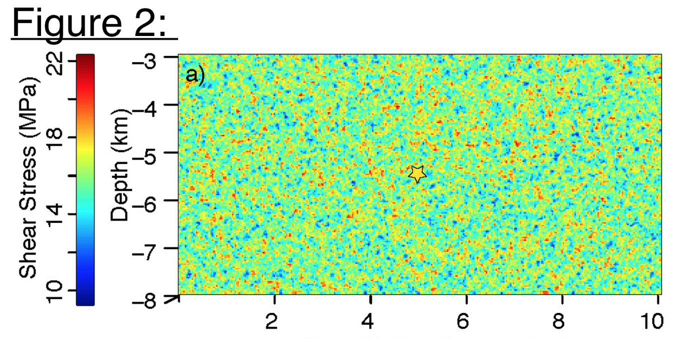

Figure 2: Example of von Karman distribution of initial shear stress on the modeled fault used to simulate induced seismicity.

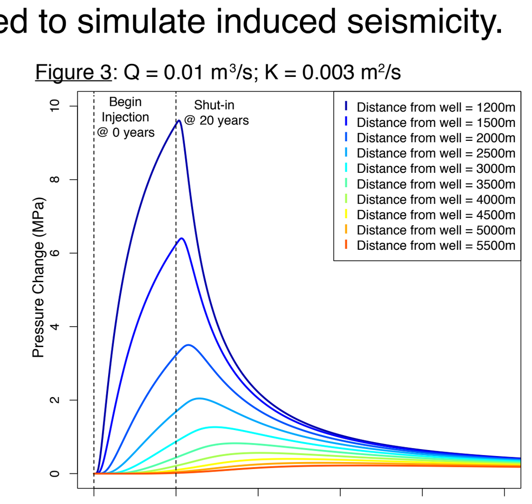

Figure 3: Example of the pore pressure change with time at different distances from the well using Eq 4. from Wang (2000) for injection between 0 and 20 years.

Variations in Injection Schedule

Is seismicity controlled by changes in peak overpressure or constant injection rate? To explore this question, we construct two simulations with the following set of parameters:

- Constant injection duration ($t = 70$ years)
- Constant injected volume ($V = 1.8 \cdot 10^7$ m^3)
- Variable injection rate
- Constant ($Q = 0.008$ m^3/s)
- Periodic ($Q = 0.014$ m^3/s)

Figure 4:

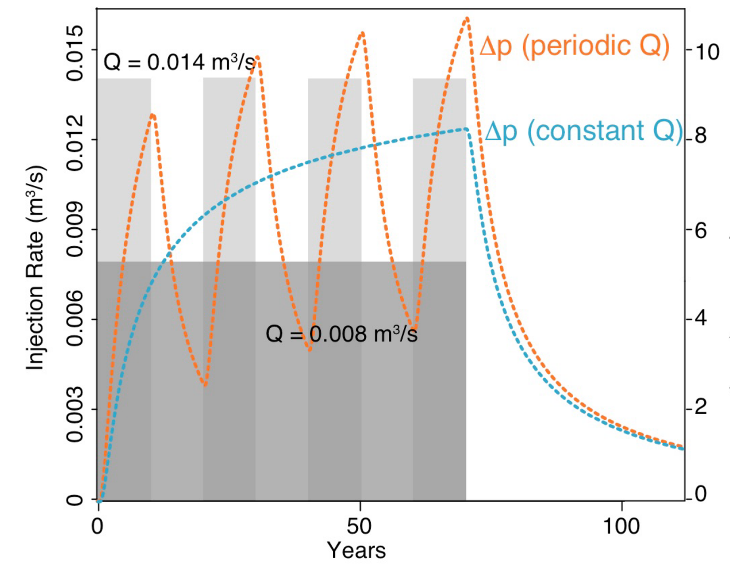

Figure 4 ▶: Overpressure for two injection schedules. Overpressure (blue dashed line) resulting from constant, low injection history (dark gray shaded region). Overpressure (orange dashed line) resulting from periodic cycling of high injection rates (periods of injection shown by light gray shaded regions).

Resulting Induced Seismicity Sequences

Figure 5:

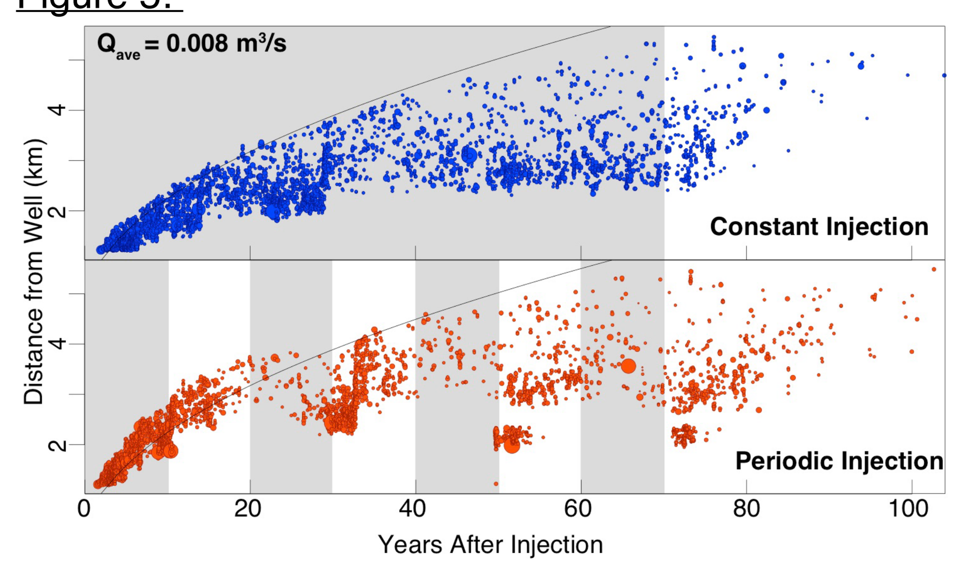

Figure 5 ◀: Hypocentral distance as a function of time resulting from constant injection rates (top) and periodic injection rates (bottom). Injection periods are shown in the gray background. Diffusivity front from Eq. 4 is shown for reference in each figure. Aftershocks from large events extend farther than the extent of the pore-pressure change.

Figure 6:

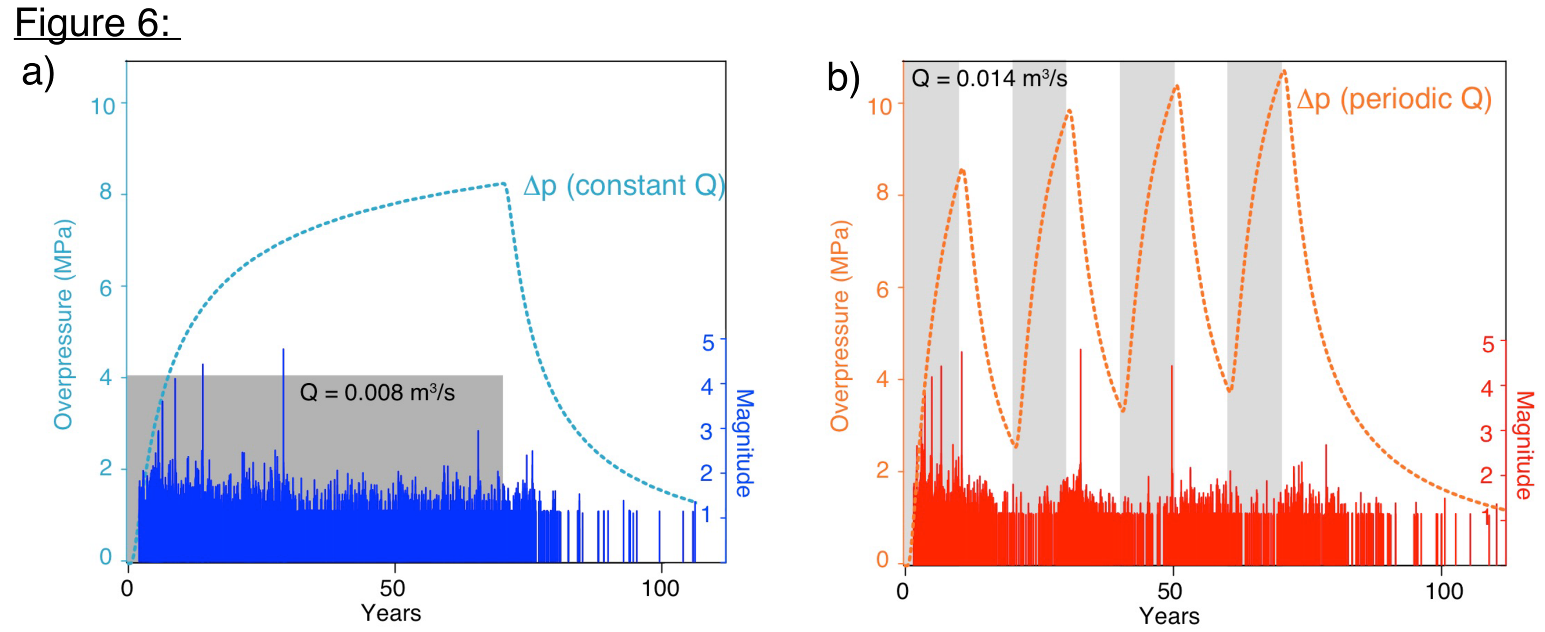

Figure 6: The distribution of earthquake magnitudes with time for each injection history. a) Resulting seismicity (blue) from the constant injection history (gray shaded region), and overpressure (blue dashed line). b) Earthquake magnitudes with time (red) for the periodic injection history (gray shaded regions) due to pore-pressure changes (orange dashed line).

Figure 7:

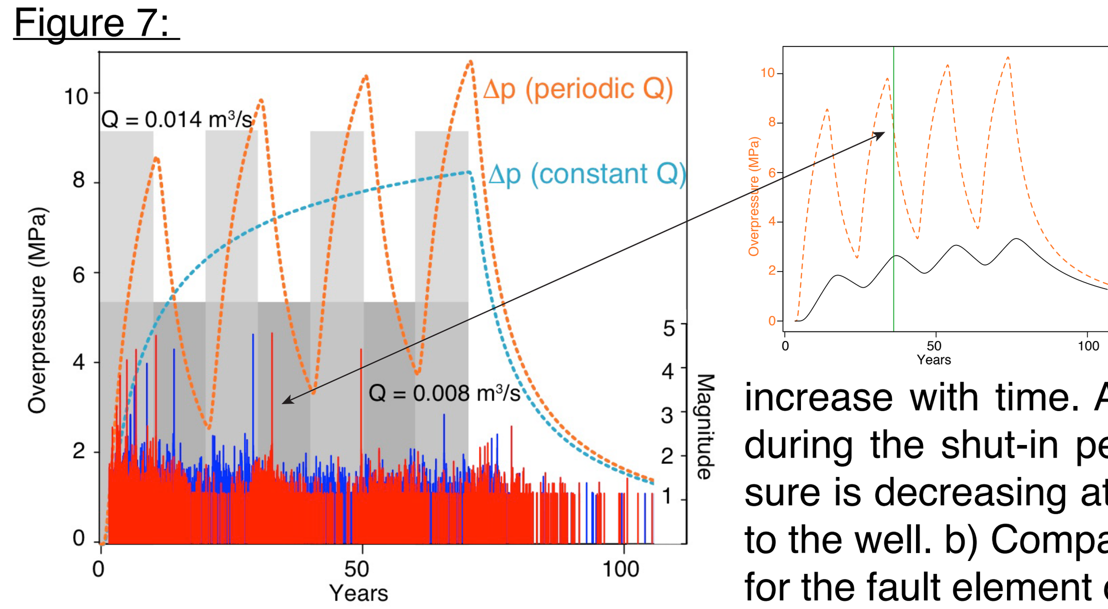

Figure 7: Comparison of the distribution of earthquake magnitudes with time for two injection schedules. For both sequences, the maximum earthquake magnitudes increase with time. At least one event occurs during the shut-in period, while the overpressure is decreasing at the fault element closest to the well. b) Comparison of the overpressure for the fault element closest to the well and the hypocentral element.

Figure 8:

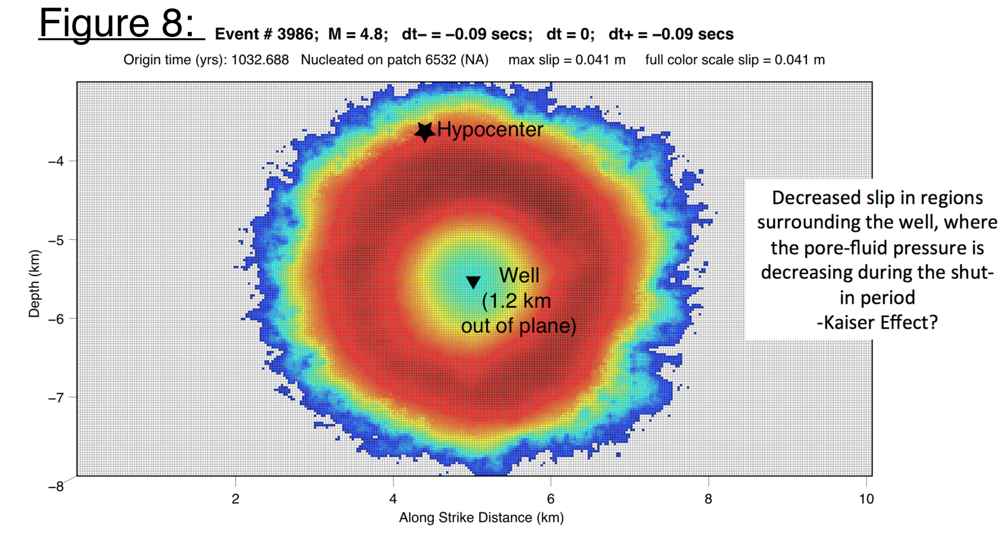

Figure 8 ◀: Slip distribution during the M4.8 event that occurs during the shut-in period, demonstrated in Figures 6b and 7. Warmer colors show maximum slip. Slip during the event is decreased in the region surrounding the well where the pore-fluid pressure is decreased, similar to the Kaiser effect.

Figure 9:

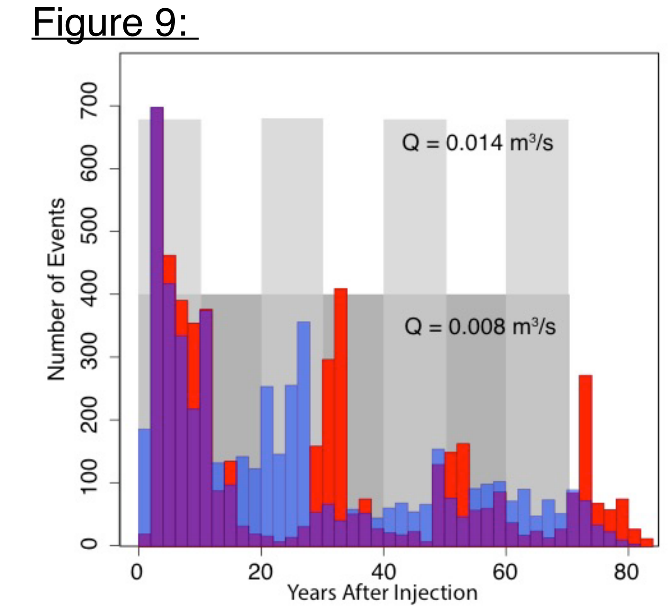

Figure 9: Histograms comparing the number of events in 2 year bins that result from each injection schedule; constant injection (blue) and periodic injection (red) (Overlapping bins, where the number of events for the constant injection history are the same as those from periodic injection history are purple).

Figure 10:

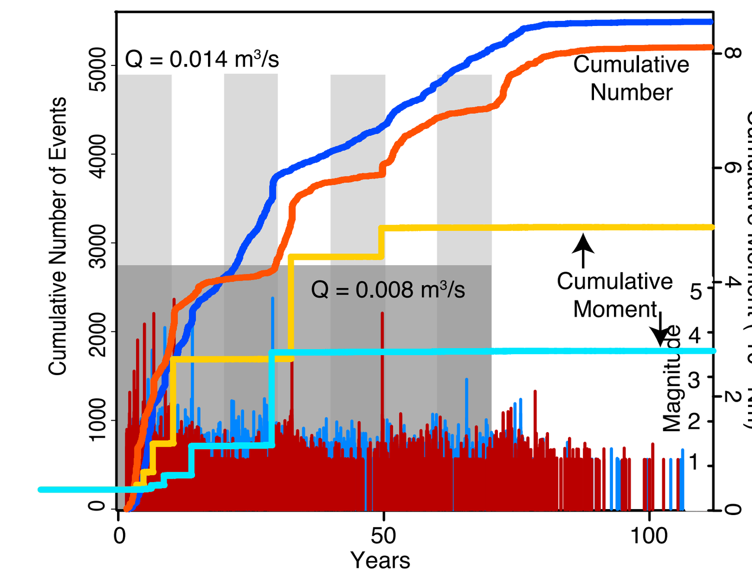

Figure 10: Comparison between the earthquake magnitudes, cumulative number of events, and cumulative seismic moment with time for the constant injection history (blue colors) and the periodic injection history (red colors). Periodic injection rates result in fewer total events, but larger magnitudes that leads to a larger total moment release.

Figure 11:

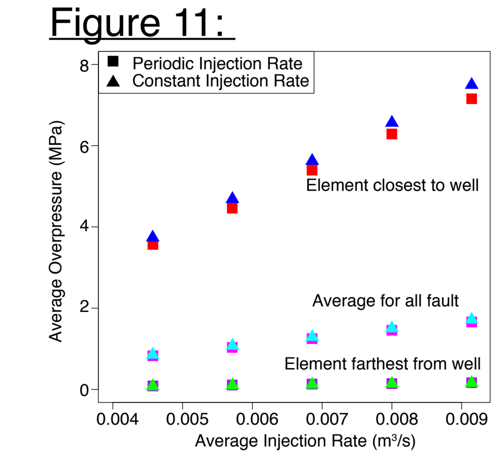

Figure 11: Comparison of the average overpressure for both injection histories for different fault elements at increasing distances from the well.

Figure 12:

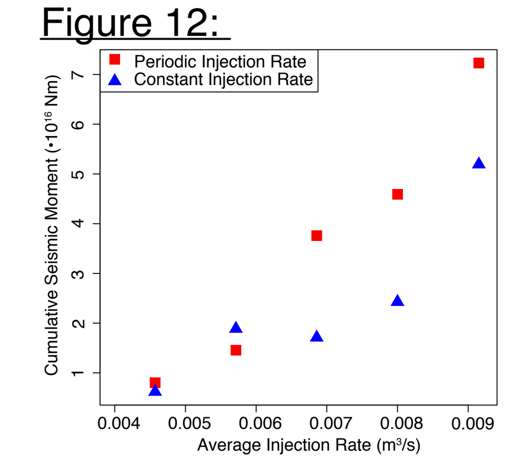

Figure 12: Comparison of the cumulative seismic moment for each injection history, showing larger moment release for the periodic injection history in general.

Figure 13:

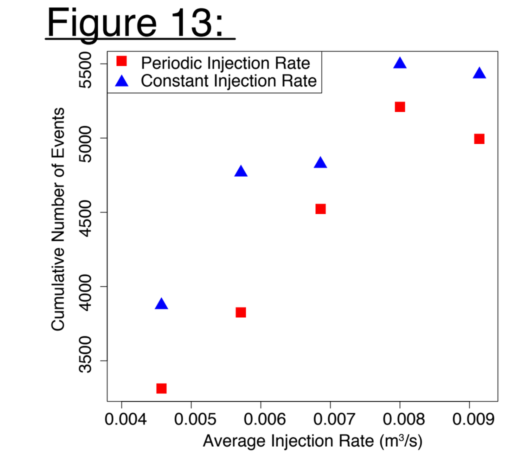

Figure 13: Comparison of the cumulative total number of events for each injection history, showing more events for the constant injection history.

Figure 14:

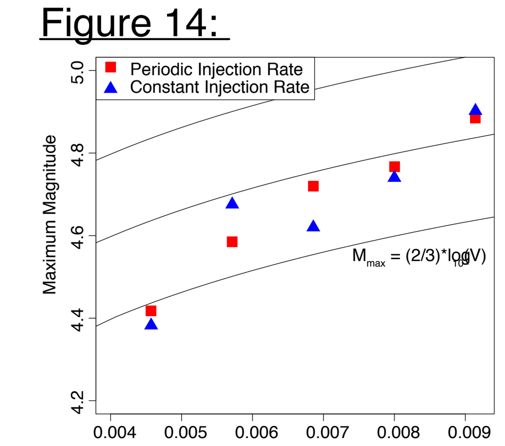

Figure 14: Comparison of the maximum event magnitude in each catalog for both injection histories. Curves show the relationship between maximum magnitude and total injection volume described by Dieterich *et al.*, 2015. The maximum magnitude increases with increasing injection rate, but appears to be uncorrelated with type of inject history.

Figure 15:

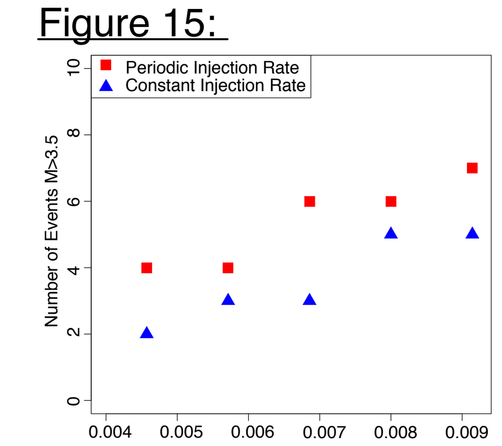

Figure 15: Comparison of the number of M>3.5 events for constant and periodic injection histories showing more large events for the periodic injection history.

Figure 16:

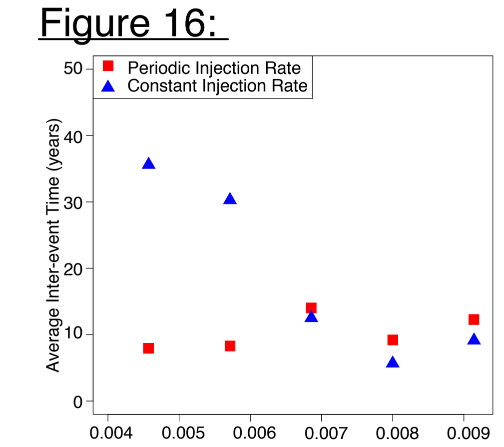

Figure 16: Comparison of the time between magnitude M>3.5 events (i.e. inter-event time) that shows decreasing inter-event times with increased injection rate for the constant injection history, but fairly uniform inter-event times for periodic injection history. Inter-event times are shorter in general with the periodic injection history.